JOURNAL OF PROPULSION AND POWER
Vol. 23, No. 5, September–October 2007

Nitrogen Oxide ($NO/NO_2/HONO$) Emissions Measurements in Aircraft Exhausts

Joda Wormhoudt,* Scott C. Herndon,* Paul E. Yelvington,† and Richard C. Miake-Lye‡
Aerodyne Research, Inc., Billerica, Massachusetts 01821
and
Changlie Wey§
QSS Group, Inc., Cleveland, Ohio 44135

DOI: 10.2514/1.23461

We present measurements of the emissions of the nitrogen oxide species nitric oxide, nitrogen dioxide, and nitrous acid in aircraft engine exhausts. In the Aircraft Particle Emissions Experiment test series, NO_x (sum of nitric oxide and nitrogen dioxide) emissions were consistent with International Civil Aviation Organization certification measurements for a CFM56-2C1 engine, and the NO_x emission index increases with increasing engine thrust. At low powers, nitrogen dioxide represents up to 80% of the total NO_x emissions for that engine, but this fraction decreases to 7% at the highest thrust setting. Nitrous acid, though a minor constituent (up to 7%) compared with NO_x, is in part formed in the turbine through reaction with hydroxyl radical. It is therefore a sensitive monitor of exhaust chemistry through which chemical kinetic models capable of predicting concentrations of other important species, such as oxides of sulfur, can be validated. The CFM56 nitrous acid measurements are compared with previous observations, and a strong dependence on engine type is observed for both the nitrous acid emission index and its contribution to the emission index of the sum of all reactive gaseous nitrogen oxides. The nitrous acid emission index increases with increasing engine thrust, but the ratio of emission indexes of nitrous acid to nitrogen dioxide decreases with increasing thrust for the CFM56.

Nomenclature

MW_t	=	molecular weight of a trace gas
n	=	number of measurements
Z	=	coefficient from the Student's t table
σ	=	standard deviation in a set of repeated measurements

Introduction

FOR more than ten years, concerns over the environmental effects of aircraft exhausts [1–5] have motivated a series of measurements of the trace gas and particulate emissions of aircraft. Included in these programs has been the development and application of a wide variety of new measurement techniques. This is the case even in the measurements reported here, of nitrogen oxides, an area in which conventional techniques are well established. The results presented here were obtained in a series of tests in which sampling probes delivered exhaust to an array of trace gas and particulate measurement instruments, including conventional NO_x (sum of nitric oxide and nitrogen dioxide) analyzers and tunable infrared differential absorption (TILDAS) instruments capable of measuring a variety of gas-phase species including nitric oxide (NO), nitrogen dioxide (NO_2), and nitrous acid (HONO) [6–10]. These sampling studies follow earlier measurement programs which used line-of-sight laser absorption [11–14].

Tunable laser absorption spectroscopy has several advantages over conventional trace gas measurement methods, including fast time response allowing transient measurements, and a first-principles calibration based on tabulated infrared line strengths. However, in the data sets treated in this paper, the major new capability brought by the laser instruments is the sensitivity and species specificity to measure concentrations of HONO. Although HONO is a relatively small fraction of the total NO_y (NO_y denotes the sum of all reactive gaseous nitrogen oxides) emission at any engine power setting, it has considerable importance as a diagnostic of the reactive trace species evolution in aircraft engine exhausts [7]. Brundish et al. [7] compares the first HONO observations, made at the NASA/QinetiQ tests, with detailed fluid dynamic/chemical kinetic modeling calculations. The clearest observed trend presented there was a substantial increase in HONO downstream of the combustor. Model calculations including HONO production by NO oxidation via the hydroxyl (OH) radical agreed with observed HONO concentrations to within the uncertainty of the measurements, suggesting that the model is valid not only for HONO but for other species whose evolution is governed by OH. It is a major purpose of the present paper to put those first observations in the context of data obtained in subsequent tests, in which different engines, more power settings, and different sampling distances behind the engine were used.

Measurement Instrumentation

We will describe in detail the nitrogen oxide measurement instrumentation used in the APEX (Aircraft Particle Emissions Experiment) carried out on 23–29 August 2004 at NASA Dryden Flight Research Center. Instrumentation similar in concept, though differing in many details, was used in the NASA/QinetiQ [6,7] and EXCAVATE [8–10] test programs whose data sets will be presented here as points of comparison to the larger APEX data set (and similar instrumentation was again used in the JETS/APEX2 and APEX3 tests, the results of which will be presented in future papers).

Measurements were made behind one of the CFM56-2C1 engines of the NASA Dryden DC-8-72 Airborne Laboratory Program aircraft. The aircraft was held in a fixed position on the tarmac, and could only be operated at high powers when crosswinds and tailwinds were negligible (although intended to protect the aircraft, this had the effect of aiding sample collection at downstream positions). Sampling probes were located at 1, 10, and 30 m behind

Received 24 February 2006; revision received 12 February 2007; accepted for publication 19 February 2007.

*Principal Scientist, 45 Manning Road, Billerica, MA 01821.
†Senior Engineer, 45 Manning Road, Billerica, MA 01821.
‡Principal Scientist, 45 Manning Road, Billerica, MA 01821. Member AIAA.
§Senior Research Scientist, 21000 Brookpark Road, Cleveland, OH 44135.

the engine exit plane. The exhaust had been substantially cooled and diluted by mixing with the atmosphere by the time it was sampled by the 30 m probe, and so this sample could be used directly without any measures (such as further dilution or heating of the sample line) to prevent water vapor condensation. The 10 m probe was an intermediate case, with samples sometimes used undiluted and sometimes being diluted with nitrogen by factors of up to 15. Sampling at 1 m was done using a probe rake that carried both "gas probes" whose samples were not diluted and whose sampling lines were heated, and "particle probes" whose samples were diluted using nitrogen added at the probe tip, after which the sampling line was not heated. After preliminary mapping studies, a single probe tip from each rake was selected as providing a representative sample of the undiluted exhaust. Typically for 1 m measurements, the laser spectrometers and all the particle instrumentation received sample flow from the selected 1 m particle probe, whereas the other gaseous species instruments, including a suite of conventional gas analysis instruments operated by NASA Glenn Research Center which yielded the NO_x data reported here, received sample flow from the 1 m gas probe.

The suite of particle and trace gas measurement instruments operated by Aerodyne at APEX was housed by the Aerodyne Mobile Laboratory, a panel truck specially modified for this purpose [15–18]. A sample line entered the truck whose flow was split isokinetically into three main fractions, one directed to nondispersive infrared CO_2 measurement instruments, one to the suite of particulate characterization instruments, and one to the trace gas instruments including the TILDAS instruments making the NO_x measurements presented here.

The laser spectrometers used in APEX were based on lasers of two different types. Tunable lead-salt diode lasers (TDLs) operate in a continuous mode and at near liquid nitrogen temperatures. In addition to the aircraft exhaust measurements already cited, these TDL instruments have been applied at Aerodyne to a variety of other applications, the most relevant being measurements of atmospheric NO_x species [19–22]. The second type of laser spectrometer was based on quantum-cascade lasers (QCLs), which operate in a pulsed mode and at temperatures allowing thermoelectric cooling rather than a liquid nitrogen Dewar. APEX was the first aircraft exhaust study to use QCL instruments, but they have been applied by Aerodyne to a number of other studies, and the system descriptions already published [23,24] also apply to the instruments used at APEX.

At APEX, an Aerodyne TDL system was used to measure NO_2 in the spectral region of 1590 cm^{-1}. In a separate trailer and, as mentioned before, taking sample flow from a separate sampling probe on the rake 1 m behind the engine, NASA Glenn Research Center operated a suite of conventional trace gas measurement instruments. These included an Eco Physics CLD 700 EL two-channel chemiluminescence nitrogen oxide analyzer making measurements of NO and NO_x, and an Advanced Fuel Research AFR-2010 MultiGas FTIR system measuring a number of gases including NO_2. (Agreement with chemiluminescence analyzer NO_2 was excellent, well within 10%, so the FTIR data will not be presented separately here.) Two Aerodyne laser systems collected spectra in regions containing HONO lines, a TDL system around 1726 cm^{-1} and a QCL system around 1693 cm^{-1}.

To quantify trace gas species concentrations, the TILDAS systems perform a real-time least-squares fit to a spectral model of the laser intensity and all the absorption lines in the region being scanned. For the major species such as CO_2 and H_2O, and for species studied in our previous work, such as NO and NO_2, the spectral model parameters are easily obtainable from the high-resolution transmission molecular absorption (HITRAN) database [25]. For HONO, we use a partial line list obtained from Herman et al. [26–28] in which relative intensities have been scaled to the absolute values in the ATMOS database [29] which have been checked with more recent laboratory measurements [30,31]. The absorption lines in the TDL spectral region are those of the *trans* isomer of HONO, whereas those below 1700 cm^{-1} are those of the *cis* isomer. The line strengths we use incorporate an assumption of the equilibrium distribution of isomers (and it has been pointed out that this is a significant source of uncertainty [31]) to directly yield concentrations of the total HONO.

Error limits in TILDAS measurements of trace gases may have contributions not only from uncertainties in the spectral and thermodynamic parameters but also from the effects of overlapping absorption lines, either those of major species or of other trace species. In the tests reviewed here before APEX, the presence of strong water lines in each spectral region had both advantages (a precise wavelength reference was available even when HONO lines were not easily seen) and disadvantages (the baseline for some HONO lines is on the wing of a strong water line and so has a rapidly changing slope). The 1726 cm^{-1} region, which was the primary one used in APEX, on the other hand, had little interference from water lines, but did have a more significant interference from the trace species formaldehyde. Indeed, in our pretest planning this spectral region was only intended to provide formaldehyde measurements, and it was only during the tests that we noticed the overlapping HONO lines.

As can be seen in Fig. 1, several of the formaldehyde and HONO lines in the center of the scan overlap very closely, so that only lines at the two sides of the scan can be used for easy distinction of which species is a major one. It can also be seen that at high engine power, it is in fact HONO that is the major contributor to the spectrum, whereas at low engine power it is formaldehyde. Once again, this spectral overlap leads to advantages and disadvantages: we get two trace species concentrations from a single laser measurement, but for some engine powers the uncertainties in one species concentration or the other are larger. Still, this "bonus" turned out to be very welcome, because the originally planned 1693 cm^{-1} region QCL suffered from

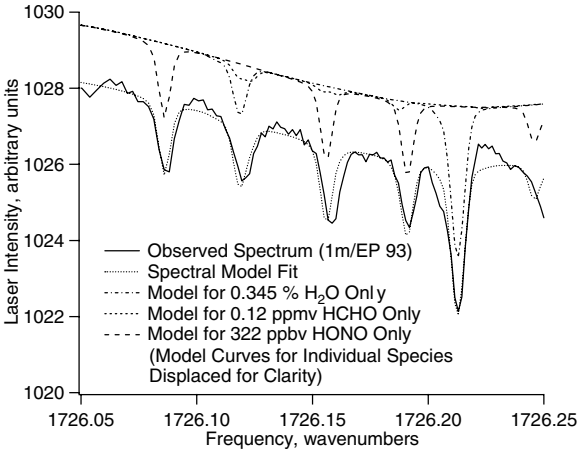

a) High engine power setting, 93% of rated thrust (HONO predominates)

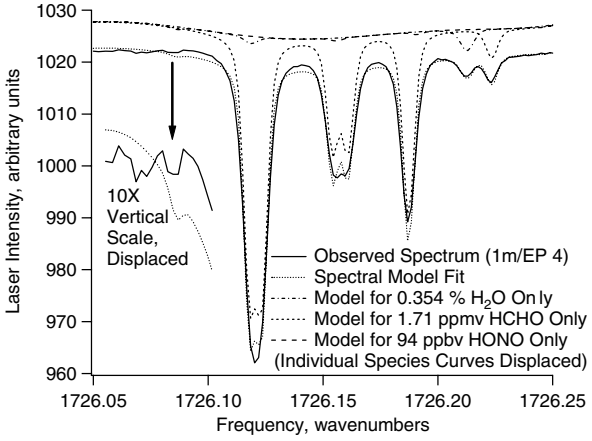

b) Low engine power setting, 4% of rated thrust (formaldehyde predominates)

Fig. 1 Primary spectral region for TDL spectrometer measurements of HONO and formaldehyde at APEX tests.

a malfunctioning temperature controller during this test, yielding data which were useful for confirming the TDL results but which had much higher signal-to-noise ratios.

Trace gas levels are reported as emission indices, where an emission index (EI) is the grams of trace gas emitted per kg of fuel consumed. The fuel consumption and CO_2 emission are proportional, and so we can derive trace gas emission indices from the trace gas concentration and CO_2 concentration observed in our sample. The CO_2 concentration we use must have the contribution due to ambient CO_2 subtracted out, and if the sample has been diluted, that dilution factor must be known before the subtraction of the ambient CO_2 can be carried out. The formula we use to convert trace gas concentrations in parts per million by volume (ppmv) is

$$\text{Emission index (trace gas)} = \frac{3160 MW_t(\text{trace gas concentration, ppmv})}{44.01[(\text{CO}_2\text{ concentration, ppmv}) - (\text{ambient CO}_2\text{, ppmv})/\text{dilution}]}$$

where 3160 is the CO_2 emission index, g CO_2 per kilogram of fuel, and 44.01 is the molecular weight of CO_2. For the emission index of nitrogen oxides, NO, NO_2, and HONO, MW_t is taken to be 46.01, that is, the NO and HONO emission indices are reported as equivalent g NO_2 per kilogram of fuel. In cases where the sample was not diluted, we subtracted an ambient CO_2 concentration of 380 ppmv, whereas for samples which were diluted by a factor of two, we subtracted 190 ppmv, and so on. For some of the 10 and 30 m sampling data, where fluctuations in observed concentrations were large, a different procedure was used in which a regression of trace gas concentration against CO_2 concentration was used to simultaneously derive the emission index (from the slope) and the term "(ambient CO_2, ppmv)/dilution" (from the intercept). For time histories in which the relative variance of the trace gas concentration is large, this is the preferred method, whereas when the relative variance is small, it is preferable to average the records of trace gas and CO_2 concentrations over the time for a given engine condition and use the averages in the preceding formula.

Results

As a first example of the nitrogen oxide measurements at APEX, Fig. 2 presents a summary of the results from the 1 m sampling position for NO (measured by NASA Glenn Research Center), NO_2, and HONO (both from the Aerodyne TDL measurements), as a function of engine power. Each contribution is added to the ones below it, so the upper boundary of the shaded area is the sum of NO + NO_2 + HONO (and therefore an approximation to NO_y, the total of all gaseous nitrogen oxide species). Error limits for these instruments will be addressed in subsequent figures. A semilog scale is used in Fig. 2 to allow the magnitude of each contribution to be readable, because throughout much of the engine power range the emissions of these three species each differ by the better part of an order of magnitude. Also shown in Fig. 2 are the nominal NO_x emission index values from the ICAO (International Civil Aviation Organization) database [32]. Good agreement between the ICAO total NO_x and APEX NO_y emission indices (within 10%) is seen at each power setting.

To consider examples of the uncertainties in the data of Fig. 2, we turn to Fig. 3, which presents NO_2 emission index measurements at the 1 m sampling point in APEX, now of three types: the Aerodyne TDL measurements on samples taken with the particle probe (the data set shown in Fig. 2), the results of the few Aerodyne TDL measurements taken with samples from the 1 m gas probe, and the NASA Glenn Research Center values (differences between measured NO_x and NO), also measured through the gas probe at 1 m. For each data point, bars indicate the size of 95% confidence limits in the mean. Considering random errors alone, we would estimate these confidence limits by $Z\sigma/n^{1/2}$ where Z [33] is 1.64487 for very large n and larger for smaller values of n. To generate the error limits in Fig. 3, we added an estimate of systematic errors of 5%, independent of number of samples or measurement technique. The resulting error limits on the TDL/particle probe points range from 7 to 23% of the means. The error limits for the NASA Glenn NO_2 measurements range from 5 to 13% of the means (at low powers, the absolute standard deviations in NASA Glenn NO values are similar to those contributing to the error bars shown for NO_2, whereas at throttle settings above 15%, the relative standard deviations in NASA Glenn NO data sets range from 3 to 6%). The large error bars for several of the Aerodyne TDL/gas probe points are due to the very few points in these data sets.

It can be seen in Fig. 3 that for the two well-measured low-power points, throttle settings of 4 and 7% of rated thrust, the NASA Glenn and Aerodyne TDL/particle probe means differ significantly (the Aerodyne value is a bit over 33% higher in each case). Of the rest, only the 40% of rated thrust points differ significantly, with the Aerodyne value being 22% lower. It is reasonable to expect that some of the discrepancy at low powers originates in errors in calibration and analysis of the two data sets, and that some has to do with the

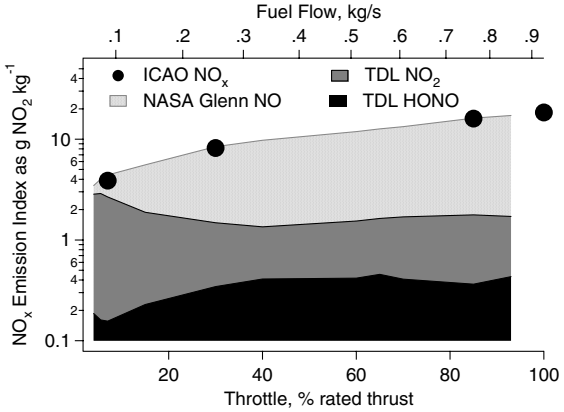

Fig. 2 Nitrogen oxide species measurements at the 1 m sampling point during the APEX tests, plotted against engine power.

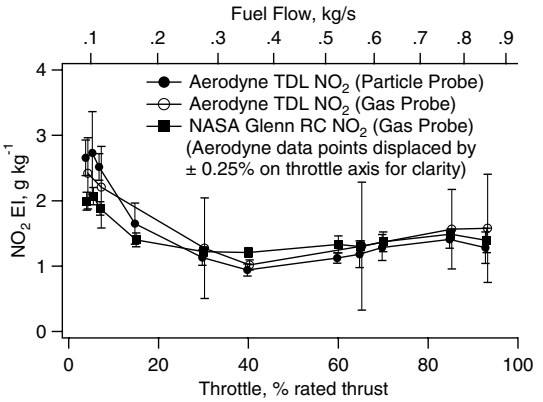

Fig. 3 NO_2 emission indices measured 1 m behind the engine during the APEX tests, plotted against engine power, by three different methods.

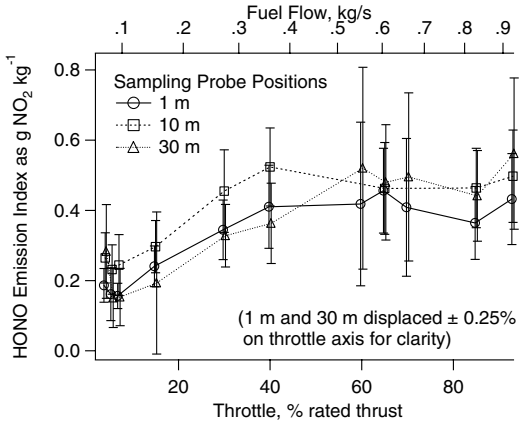

Fig. 4 HONO measurements at the APEX test for all three sampling distances behind the engine, plotted against engine power.

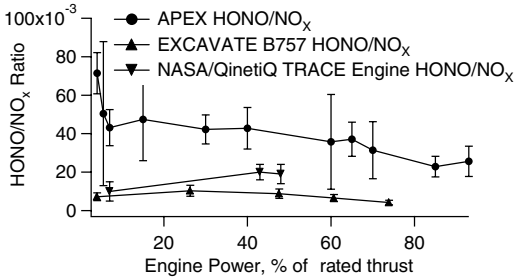

Fig. 5 Ratios of HONO and NO_x emission indices for sampling at 1 m downstream positions at three aircraft exhaust tests, plotted against engine power.

differences in the sampling probes used by the Aerodyne and NASA Glenn measurements. The fact that the Aerodyne measurements using the probe used throughout by NASA Glenn lie halfway between the other two data sets suggests that both sources contribute to the discrepancy.

Figure 4 presents the same APEX HONO at 1 m data set shown in Fig. 2, now with added error bars and with two additional data sets, the APEX measurements of samples taken at 10 and 30 m behind the engine exit plane. As before, the error bars are intended to represent 95% confidence limits in the mean, this time with the assumption of 20% systematic errors added in quadrature to estimates of random errors based on standard deviations of repeated measurements. Once again, especially large error bars are due to small numbers of repeated measurements. Because of the lower signal-to-noise ratios in the HONO spectra and the larger potential systematic errors, the error bars in Fig. 4 are substantially larger than those for NO_2 in Fig. 3. One result of these large error bars is that it is not possible to say with certainty that there is a systematic trend in HONO emission index with sampling distance behind the engine exit plane. It is clear, as previously reported [6,8–10], that HONO emissions are larger at high power than at low power. Whether there is a smaller but perhaps significant increase in HONO emission index also at the very lowest power observed relative to the low HONO levels at 5 and 7% is less certain, but a possibility.

To compare the HONO observations in the APEX test with those of previous tests, we turn to Table 1 and to Fig. 5. Table 1 begins by specifying the engines observed in each test. The QinetiQ Transport and Chemical Evaluation (TRACE) engine is a generic engine typical of CAEP 4 compliant engines currently in use, and is fitted with 10 turboannular combustors which allow flexible simulation of modern annular combustors. The Experiment to Characterize Aircraft Volatile Aerosol and Trace-Species Emissions (EXCAVATE) made measurements on the NASA Airborne Research Integrated Experiments System (ARIES) Boeing 757-200 and on the NASA Langley T-38A Talon. The ranges quoted of HONO and ratios of HONO to NO_2 and NO_x are related to the ranges of engine power settings which happened to be used in the various tests, and are not intended to replace the detailed reporting of test data in this paper and [7]. Furthermore, whereas HONO emission index has been seen to increase with increasing power, the $HONO/NO_x$ ratio typically decreases with power (and so in Table 1, $HONO/NO_x$ of 0.07 is for a throttle setting of 4%, with high power values of the ratio approaching 0.02), and, as seen in Fig. 5, the $HONO/NO_2$ ratio also is lower at higher powers. Table 1 also specifies some of the measurement details, including the source of the NO_2 and NO_x emission indices used in the ratios, and the spectroscopic details of the HONO observations. (The group making the conventional trace gas measurements of the TRACE combustor and engine was the same, but between the two tests, that group at the Defense Evaluation and Research Agency, DERA, was privatized and became part of QinetiQ, Ltd.)

It can be seen in both Table 1 and Fig. 5 that there are substantial variations in HONO emission index with engine type. In Fig. 5, the high power $HONO/NO_x$ ratio observed in APEX is more than twice the maximum observed from the 757 in EXCAVATE, and that level is in turn about twice that seen from the TRACE engine in the NASA/QinetiQ tests. But Table 1 shows the most significant difference in HONO emission with engine type, because for the Langley T-38 observed in EXCAVATE, the HONO was below the detection limit. This means that the HONO concentration in the T-38 exhaust was at least 20 times lower than the concentrations seen in high power cases with the 757. All other parameters of the two observations, the instrumentation, the sampling lines, probes, and techniques, the ambient conditions, and so forth, remained the same.

It is known that HONO formation from other nitrogen oxides on surfaces is possible, especially in the presence of water. The large change in HONO emission with engine type is one of three observations that led us to the conclusion that much of the HONO we observed is a true exhaust constituent, and is not formed in the probe or sampling line. The other two points of evidence are the reproducible trends with engine power, and the lack of significant trends with sampling position. It can be argued, on the one hand, that although the NO and NO_2 exhaust concentrations change dramatically from low to high power, and the exhaust temperatures and water contents are always in the range that could promote HONO

Table 1 HONO measurements in aircraft exhausts: ranges of observed emission indices, ratios to NO_2 and NO_x, and spectroscopic regions

TEST	NASA/QinetiQ	NASA/QinetiQ	EXCAVATE	EXCAVATE	APEX
Engine	TRACE combustor	TRACE engine	B757 RB-211-535E4 turbofan	T-38 J85-GE-5A turbojet	DC-8 CFM56-2C1 turbofan
HONO EI	0.021–0.032	0.03–0.108	0.03–0.24	<0.01[a]	0.13–0.43
$HONO/NO_2$	0.05–0.1	0.07–0.18	——	——	0.05–0.45
NO_2 values	DERA	QinetiQ	——	——	Aerodyne
$HONO/NO_x$	0.0025–0.005	0.007–0.018	0.004–0.01	——	0.2–0.07
NO_x values	DERA	QinetiQ	ICAO	——	NASA Glenn RC
HONO region frequency, cm^{-1}	1666.173	1666.173	1666.46	1666.46	1726.193 (1692.88)

[a]below detection limit at all engine powers

formation on surfaces, the HONO concentrations do not track either the NO or NO_2 concentrations, but follow their own trend, as if the measured HONO is not governed by a simple formation process in the sampling system. On the other hand, the characteristics of the exhaust sampled at the 1, 10, and 30 m points change dramatically, as the temperature, water content, and nitrogen oxide concentrations all drop, yet no dramatic change in HONO emission index is seen. If future tests produce data sets with smaller error limits, this may allow us to discern trends in HONO emission index with sampling position, and that in turn may allow the estimation of contributions from formation in the probe and/or sampling line to the observed HONO.

Summary

Whereas at higher powers aircraft NO_x is dominated by NO, at low powers NO_2 can contribute more than 80% of the total NO_x. HONO can also be significant (up to 7% of NO_x in the observations presented here). More important, HONO can be a useful diagnostic of exhaust chemistry. Key assumptions underlying this statement are that observed HONO concentrations are representative of the true exhaust composition, and that differences in engine chemistry are indeed manifested as differences in HONO emissions. The work presented here documenting measurements of NO, NO_2, and HONO for a variety of engines, power levels, and sampling distances provides support for both assumptions.

Acknowledgments

The primary work reported here was carried out with funding from the University of Missouri Center of Excellence for Aerospace Particulate Emissions Reduction Research (NASA Cooperative Agreement NCC3-1084) under University of Missouri–Rolla Subcontract No. 000729-02. The entire presented results represent the successful teamwork carried out under three different field missions: NASA/QinetiQ, EXCAVATE, and APEX, and we are indebted to our colleagues at QinetiQ, NASA, and University of Missouri–Rolla for the collaborative efforts that allowed these measurements to be made. For the APEX mission, the entire APEX measurement team contributed to its success and enabled this analysis.

References

[1] Stolarski, R. S., and Wesoky, H. L. (eds.), *Atmospheric Effects of Stratospheric Aircraft: A Fourth Program Report*, NASA, Reference Publ. 1359, Washington, D.C., 1995.

[2] Stolarski, R. S., Baughcum, S. L., Brune, W. H., Douglass, A. R., Fahey, D. W., Friedl, R. R., Liu, S. C., Plumb, R. A., Poole, L. R., Wesoky, H. L., and Worsnop, D. R., *1995 Scientific Assessment of the Atmospheric Effects of Stratospheric Aircraft*, NASA, Reference Publ. 1381, Washington, D.C., 1995.

[3] Friedl, R. (ed.), *Atmospheric Effects of Subsonic Aircraft: Interim Assessment Report of the Advanced Subsonic Technology Program*, NASA Reference Publ. 1400, Washington, D.C., 1997.

[4] Wine, P., Carrier, G., Erickson, D., III, Krull, N., McConnell, J., Mirabel, P., Oppenheimer, M., Rosenlof, K., Russell, L., and Spicer, C., *Review of NASA's Atmospheric Effects of Stratospheric Aircraft Project*, National Research Council, National Academy Press, Washington, D.C., 1999.

[5] Kaehn, A. J., Calvert, J. G., Carrier, G. F., Clarke, A. D., Ehhalt, D. H., Erickson, D. J., III, Granier, C., Greitzer, E. M., Mirabel, P., Oppenheimer, M., Slinn, W. G. N., and Stamnes, K., *Atmospheric Effects of Aviation: A Review of NASA's Subsonic Assessment Project*, National Research Council, National Academy Press, Washington, D.C., 1999.

[6] Whitefield, P. D., Hagen, D. E., Wormhoudt, J. C., Miake-Lye, R. C., Wilson, C., Brundish, K., Waitz, I., Lukachko, S., and Yam, C. K., "NASA/QinetiQ Collaborative Program: Final Report," NASA CR-2002-211900, Sept. 2002.

[7] Brundish, K., Clague, A. R., Miake-Lye, R. C., Brown, R. C., Wormhoudt, J., Lukachko, S. P., Chobot, A. T., Yam, C. K., Waitz, I. A., Hagen, D. E., and Whitefield, P. D., "Evolution of Carbonaceous Aerosol and Aerosol Precursor Emissions through a Gas Turbine Engine," *Journal of Propulsion and Power* (in this issue).

[8] Anderson, B. E., Winstead, E., Hudgins, C., Plant, J., Branham, H.-S., Thornhill, L., Boudries, H., Canagaratna, M., Miake-Lye, R., Wormhoudt, J., Worsnop, D., Miller, T., Ballenthin, J., Hunton, D., Viggiano, A., Pui, D., Han, H.-S., Blake, D., and McEchern, M., "Overview of Results from the NASA Experiment to Characterize Aircraft Volatile Aerosol and Trace Species Emissions (EXCAVATE)," *Proceedings of the AAC-Conference, 30 June–3 July 2003, Friedrichshafen, Germany*, European Commission, Luxembourg, Germany, Air Pollution Research Rept. 83, 2004, pp. 27–36.

[9] Boudries, H., Wormhoudt, J., Worsnop, D., Canagaratna, M., Onasch, T., Miake-Lye, R., and Anderson, B., "Aerosol and Gas Chemistry of Commercial Aircraft Emissions Measured in the NASA EXCAVATE Program," *Proceedings of the AAC-Conference, 30 June–3 July 2003, Friedrichshafen, Germany*, European Commission, Luxembourg, Germany, Air Pollution Research Rept. 83, 2004, pp. 85–90.

[10] Anderson, B. E., Branham, H.-S., Hudgins, C. H., Plant, J. V., Ballenthin, J. O., Miller, T. M., Viggiano, A. A., Blake, D. R., Boudries, H., Canagaratna, M., Miake-Lye, R. C., Onasch, T., Wormhoudt, J., Worsnop, D., Brunke, K. E., Culler, S., Penko, P., Sanders, T., Han, H.-S., Lee, P., Pui, D. Y. H., Thornhill, K. L., and Winstead, E. L., "Experiment to Characterize Aircraft Volatile Aerosol and Trace-Species Emissions (EXCAVATE)," NASA TM-2005-213783, Aug. 2005.

[11] Wormhoudt, J., Zahniser, M. S., Nelson, D. D., McManus, J. B., Miake-Lye, R. C., and Kolb, C. E., "Infrared Tunable Diode Laser Measurements of Nitrogen Oxide Species in an Aircraft Engine Exhaust," *Optical Techniques in Fluid, Thermal, and Combustion Flow (Proceedings of SPIE: The International Society for Optical Engineering)*, Vol. 2546, Society of Photo-Optical Instrumentation Engineers, Bellingham, WA, 1995, pp. 552–561.

[12] Miake-Lye, R., Wormhoudt, J., Howard, R., and Hiers, R., Jr., "Aircraft Engine Emissions Measurements at Simulated Flight Altitude Conditions," AIAA Paper 97-3379, July 1997.

[13] Miake-Lye, R. C., and Wormhoudt, J., "Emission Measurements in Aircraft Engine Exhausts Using Tunable Diode Laser Infrared Absorption," *ISABE—International Symposium on Air Breathing Engines, 13th, Chattanooga, TN, 7–12 Sept. 1997, Proceedings,* , Vol. 2, AIAA A97-38891 10-07, Reston, VA, 1997, pp. 1109–1119.

[14] Berkoff, T. A., Wormhoudt, J., and Miake-Lye, R. C., "Measurement of SO_2 and SO_3 Using a Tunable Diode Laser System," *Environmental Monitoring and Remediation Technologies (Proceedings of SPIE: The International Society for Optical Engineering)*, Vol. 3534, Society of Photo-Optical Instrumentation Engineers, Bellingham, WA, 1999, pp. 686–688.

[15] Kolb, C. E., Herndon, S. C., McManus, J. B., Shorter, J. H., Zahniser, M. S., Nelson, D. D., Jayne, J. T., Canagaratna, M. R., and Worsnop, D. R., "Mobile Laboratory with Rapid Response Instruments for Real-Time Measurements of Urban and Regional Trace Gas and Particulate Distributions and Emission Source Characteristics," *Environmental Science and Technology*, Vol. 38, No. 21, 2004, pp. 5694–5703.

[16] Herndon, S. C., Shorter, J. H., Zahniser, M. S., Nelson, D. D., Jayne, J., Brown, R. C., Miake-Lye, R., Waitz, I., Silva, P., Lanni, T., Demerjian K., and Kolb, C. E., "NO and NO_2 Emission Ratios Measured from In-Use Commercial Aircraft During Taxi and Take-Off," *Environmental Science and Technology*, Vol. 38, No. 22, 2004, pp. 6078–6084.

[17] Herndon, S. C., Jayne, J. T., Zahniser, M. S., Worsnop, D. R., Knighton, B., Alwine, E., Lamb, B. K., Zavala, M., Nelson, D. D., McManus, J. B., Shorter, J. H., Canagaratna, M. R., Onasch, T. B., and Kolb, C. E., "Characterization of Urban Pollutant Emissions Fluxes and Ambient Concentration Distributions Using a Mobile Laboratory with Rapid Response Instrumentation," *Atmospheric Chemistry (Faraday Discussions)*, Vol. 130, Royal Society of Chemistry, Cambridge, England, UK, 2005, pp. 327–339.

[18] Jiang, M., Marr, L. C., Dunlea, E. J., Herndon, S. C., Jayne, J. T., Kolb, C. E., Knighton, W. B., Rodgers, T. M., Zavala, M., Molina, L. T., and Molina, M. J., "Vehicle Fleet Emissions of Black Carbon, Polycyclic Aromatic Hydrocarbons, and Other Pollutants Measured by a Mobile Laboratory in Mexico City," *Atmospheric Chemistry and Physics*, Vol. 5, No. 18, 2005, pp. 3377–3387.

[19] Zahniser, M. S., Nelson, D. D., McManus, J. B., and Kebabian, P. L., "Measurement of Trace Gas Fluxes Using Tunable Diode Laser Spectroscopy," *Philosophical Transactions of the Royal Society of London*, Vol. A351, No. 1696, 1995, pp. 371–381.

[20] Nelson, D. D., Jr., Zahniser, M. S., McManus, J. B., Kolb, C. E., and Jimenez, J. L., "Tunable Diode Laser System for the Remote Sensing of On-Road Vehicle Emissions," *Applied Physics B (Lasers and Optics)*, Vol. 67, No. 4, 1998, pp. 433–441.

[21] Nelson, D. D., Jimenez, J. L., McRae, G. J., Zahniser, M. S., and Kolb, C. E., "Remote Sensing of NO and NO_2 Emissions from Heavy-Duty Diesel Trucks Using Tunable Diode Lasers," *Environmental Science*

and Technology, Vol. 34, No. 11, 2000, pp. 2380–2387.

[22] Shorter, J. H., Herndon, S., Zahniser, M. S., Nelson, D. D., Wormhoudt, J., Demerjian, K. L., and Kolb, C. E., "Real-Time Measurements of Nitrogen Oxide Emissions from In-Use New York City Transit Buses Using a Chase Vehicle," *Environmental Science and Technology*, Vol. 39, No. 20, 2005, pp. 7991–8000.

[23] Nelson, D. D., McManus, B., Urbanski, S., Herndon, S., and Zahniser, M. S., "High Precision Measurements of Atmospheric Nitrous Oxide and Methane Using Thermoelectrically Cooled Mid-Infrared Quantum Cascade Lasers and Detectors," *Spectrochimica Acta, Part A: Molecular Spectroscopy*, Vol. 60, No. 14, 2004, pp. 3325–3335.

[24] Jimenez, R., Herndon, S., Shorter, J. H., Nelson, D. D., McManus, J. B., and Zahniser, M. S., "Atmospheric Trace Gas Measurements Using a Dual Quantum-Cascade Laser Mid-Infrared Absorption Spectrometer," *Novel In-Plane Semiconductor Lasers IV (Proceedings of SPIE: The International Society for Optical Engineering)*, Vol. 5738, Society of Photo-Optical Instrumentation Engineers, Bellingham, WA, 2005, pp. 318–331.

[25] Rothman, L. S., Jacquemart, D., Barbe, A., Benner, D. C., Birk, M., Brown, L. R., Carleer, M. R., Chackerian, C., Jr., Chance, K., Coudert, L. H., Dana, V., Devi, V. M., Flaud, J.-M., Gamache, R. R., Goldman, A., Hartmann, J.-M., Jucks, K. W., Maki, A. G., Mandin, J.-Y., Massie, S. T., Orphal, J., Perrin, A., Rinsland, C. P., Smith, M. A. H., Tennyson, J., Tolchenov, R. N., Toth, R. A., Vander Auwera, J., Varanasi, P., and Wagner, G., "HITRAN 2004 Molecular Spectroscopic Database," *Journal of Quantitative Spectroscopy and Radiative Transfer*, Vol. 96, No. 2, 2005, pp. 139–204.

[26] Melen, F., and Herman, M. J., "Vibrational Bands of $H_xN_yO_z$ Molecules," *Journal of Physical and Chemical Reference Data*, Vol. 21, No. 4, 1992, pp. 831–881.

[27] Guilmot, J.-M., Melen, F., Herman, M., "Rovibrational Parameters for cis-Nitrous Acid," *Journal of Molecular Spectroscopy*, Vol. 160, No. 2, 1993, pp. 401–410.

[28] Guilmot, J.-M., Godefroid, M., and Herman, M., "Rovibrational Parameters for trans-Nitrous Acid," *Journal of Molecular Spectroscopy*, Vol. 160, No. 2, 1993, pp. 387–400.

[29] Brown, L. R., Farmer, C. B., Rinsland, C. P., and Toth, R. A., "Molecular Line Parameters for the Atmospheric Trace Molecule Spectroscopy Experiment," *Applied Optics*, Vol. 26, No. 23, 1987, pp. 5154–5181.

[30] Becker, K. H., Kleffman, J., Kurtenbach, R., Wiesen, P., Febo, A., Gherardi, M., and Sparapani, R., "Line Strength Measurements of trans-HONO near 1255 cm^{-1} by Tunable Diode Laser Spectrometry," *Geophysical Research Letters*, Vol. 22, No. 18, 1995, pp. 2485–2488.

[31] Barney, W. S., Wingen, L. M., Lakin, M. J., Brauers, T., Stutz, J., and Finlayson-Pitts, B. J., "Infrared Absorption Cross-Section Measurements for Nitrous Acid (HONO) at Room Temperature," *Journal of Physical Chemistry A*, Vol. 104, No. 8, 2000, pp. 1692–1699.

[32] Anon., ICAO Exhaust Emissions Data Bank, Sheet 1RR013, 1 Oct. 2004, (test dates 2 July 1984–25 Oct. 1984), http://www.caa.co.uk/docs/702/1RR013_01102004.pdf [retrieved 15 Feb. 2006].

[33] Abramowitz, M., and Stegun, I. A., *Handbook of Mathematical Functions*, Dover, New York, 1965.

L. Maurice
Associate Editor